Robotica (2023), **41**, pp. 1617–1633
doi:10.1017/S0263574723000024

CAMBRIDGE UNIVERSITY PRESS

RESEARCH ARTICLE

Comparison of theoretical and experimental models for knee flexion/extension using a cable-driven robot

Rogério S. Gonçalves* and Yasmin V. Kaufmann

School of Mechanical Engineering, Federal University of Uberlândia, Uberlândia, Brazil
*Corresponding author. E-mail: rsgoncalves@ufu.br

Received: 10 September 2022; **Revised:** 5 December 2022; **Accepted:** 28 December 2022;
First published online: 19 January 2023

Keywords: robotics, mechatronic systems, rehabilitation, cable-driven robot, knee

Abstract

To support and facilitate the rehabilitation of patients with physical limitations and aid the therapist, several robotic structures are being studied. Among the structures, the cable-driven robots stand out. The cable-driven robots are structures actuated by cables and have the advantages of being flexible and reconfigurable for each patient. The objective of this paper is to develop a theoretical model for knee flexion/extension force and moment using a cable-driven robot. The proposed model is necessary for elaborating a referential to which diagnosis can be made and the improvement of the patient evaluated. The presented theoretical model was validated through experiments with twelve sedentary and healthy volunteers. The first procedure tested ten subjects in three thigh angles for knee flexion motion; the second procedure tested two subjects in flexion and extension for the same thigh angle. The results show the validity of the model for 88.58% of the tests in an ANOVA analysis with a 99% confidence interval. The similarity of data for different gender, ages, and intrinsic factors was noted, implying that the model is representative and independent of the subject's individuality. Differences between flexion and extension values were observed, which need to be studied in the future.

1. Introduction

With the advancement of technology, it became possible to apply robotics structures in several areas, in particular medicine, fields such as robotic surgery, and also in the rehabilitation of patients with disabilities and loss of movement [1].

Several types of robotic structures were tested and used for the rehabilitation of upper [2] and lower limbs [3, 4], and the cable-driven robots are the object of attention of researchers due to a series of benefits that make them suitable for rehabilitation purposes such as workspace greater than conventional parallel structures and the possibility of adaptation to different patients and therapies, easy assembly and disassembly of mechanical structure (easily transported) and, mainly, the acceptance of the patient already adapted to therapies that use ropes [5–7].

The knee is a complex joint with many structures that make it vulnerable to a variety of injuries like sprains, ligament tears, fractures, dislocations, neurological disorders, among others. Knee injuries can be treated with bracing, rehabilitation exercises, or surgery. Before and after the procedures necessary to rehabilitate the human knee, it is necessary to measure its condition. Generally, the measurement of the status of the knee is carried out using manual clinical scales measured by physiotherapists.

This paper uses the concept of biomechanics [8], to find a model of knee movement forces using a cable-driven robotic structure. This biomechanical model relies on the application of joint stiffness as a moment against body movement. Through this stiffness, it is possible to verify the existence and severity of joint deficiencies in the limbs using strength and movement assessments, in addition to verifying the improvement of the limb with the passage of treatment.

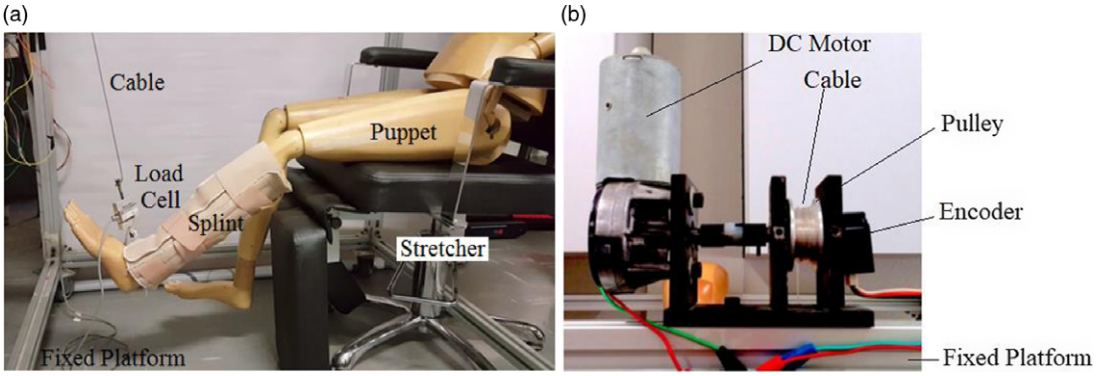

Figure 1. *(a) Cable-driven robot; (b) Traction module.*

The present paper intends to compare values of the force/moment obtained by a mechanical theoretical model with the experimental biomechanical model of knee movement and to verify the application of the theoretical model in a healthy population, using a cable-driven robot.

This study is justified by the need to support and facilitate the rehabilitation of a series of patients with limitations in knee movements through a low-cost, easy-to-use robotic system. Furthermore, it is necessary to find the validity between the theoretical and the experimental model in healthy knees for future comparisons and diagnoses in patients.

This paper is structured as follows: Section 2 provides the design of the cable-driven robot used, followed by a brief review of the knee kinesiology in Section 3. After that, the knee force and moment models are developed in Section 4. The results and discussion are presented in Section 5. Finally, the conclusion and recommendations are outlined in Section 6.

2. Design of the cable-driven robot

The parallel robotic structure actuated by cables, under development and used in this paper, acts on the patient through cables driven by electric motors coupled to encoders. The fixed platform was built with aluminum structural profiles that allow flexibility in assembly and reconfiguration of the structure, Fig. 1(a).

The cable traction module, Fig. 1(b), consists of a DC Bosch motor (CEP 006 WMO 310) with 45 rpm, 12 V, nominal torque of 10 Nm (peak 48 Nm); encoder HEDS 5500 model with 500 pulses; elastic coupling; bearings; pulley; and load cell (CSAZL 20) with a capacity of 20 kgf. The load cell measures the force in the cable directly, Fig. 1(a).

The actuators are controlled using an Arduino Mega 2560 and an Arduino Motor Shield. The Arduino is connected to the notebook via a USB interface. The load cell signals pass through a signal conditioning board for signal amplification. The cables are attached to an orthosis (mobile platform) placed on the patient who can lie down or sit in a chair.

The use of one cable is enough to perform the individual movements of knee flexion/extension and the weight of the lower limb assists in the flexion/extension movement [9]. A complete description of the mathematical model and validation of the cable-driven robot used in this paper can be found in [7, 9, 10].

3. Knee kinesiology

According to [11], the knee is the intermediate joint of the lower limb. It has one degree of freedom around the transverse axis XX', Fig. 2(a), with the possibility of flexion/extension movements in the

https://doi.org/10.1017/S0263574723000024 Published online by Cambridge University Press

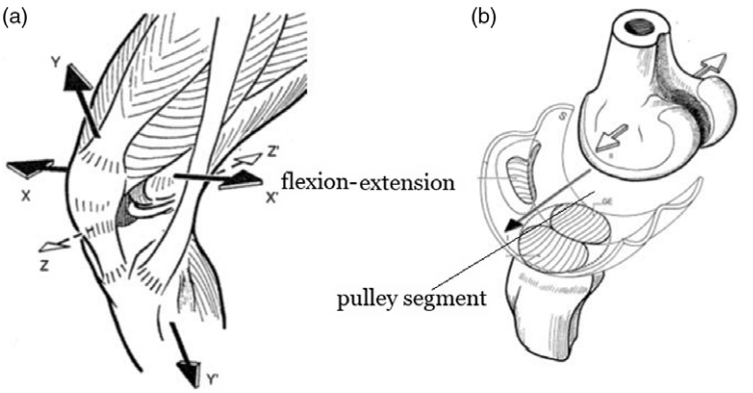

Figure 2. *(a) Knee joint movement; (b) Trochlear-type joint knee (adapted from ref.* [11]*).*

sagittal plane that allow the distance from the floor to be regulated by approaching/removing the limb end to its source. The second degree of freedom, around the longitudinal axis YY', Fig. 2(a), is possible when the knee is flexed.

In ref. [11], the kinesiology of the knee, which is capable of reconciling two contradictions: having great stability in maximum extension (where it makes great efforts due to the weight of the body) and acquiring great mobility from a given angle of flexion (necessary in running and for orientation of the foot), was discussed. Its mechanical device resolves these contradictions but is subject to dislocations and sprains. During flexion, the joint is more prone to ligament and meniscus injuries, and in extension, more vulnerable to joint fractures and ligament ruptures [12].

The knee joint in flexion/extension movement is conditioned by a trochlear-type joint, constituting a pulley or, more precisely a pulley segment, Fig. 2(b).

More complex biomechanical models are found in the literature to represent the knee. In ref. [13], a knee model based on a spatial parallel mechanism to consider translations and rotations of the knee biomechanical model was proposed. In ref. [14], a new adjustable knee joint mechanism is synthesized based on a crossed four-bar mechanism to reproduce the complex flexion/extension movement of the knee joint. Although there are more complex models to represent the human knee, the idea of this paper is to obtain a simpler, low-cost, and easier-to-use model for health professionals.

In this paper, the following data will be used: mass of the body segments in relation to the total weight of the individual according to ref. [15], Table I, and location of the center of mass of the segments (center of mass in relation to their given length in the percentage of that size) according to ref. [16], Table II.

3.1. The resistance torque in the knee joint

Due to the different structures that make up the knee, such as bones, ligaments, muscles, and menisci, the knee joint ends up offering resistance to movement. Together with the friction between the bones, these forces generate a torque against the movement performed, called the resistance torque. It can be influenced by several factors such as the individual's stretching, muscle tone, and frequency of physical activity, among others [17].

In ref. [18], the isokinetic strength test method, which performs dynamic contractions during a movement with the body velocity kept constant (isokinetic) without the influence of the force exerted by the subject, was used to find the knee torque curves. The author used a dynamometer that performs isometric, isokinetic, and isotonic tests. The results of the isokinetic tests showed a substantial improvement in the operated leg through the 8 weeks of treatment. The author indicates that this improvement in a short period may be partially due to the increase in muscle mass and neuromuscular coordination that follows

https://doi.org/10.1017/S0263574723000024 Published online by Cambridge University Press

Table I. *Data of lower limb used in this paper* [15].

Mass of body segments in relation to the total mass (%)		
	Men	**Woman**
Thigh	10.50	11.75
Leg	4.75	5.35
Foot	1.43	1.33
Leg + foot	6.18	6.68

Table II. *CM of segments (%), Dempster* [16].

Thigh (from the greater trochanter)	43.30
Leg (from the lateral epicondyle of the femur)	43.30
Foot (from the ankle)	24.90
Leg + foot	43.40

the surgery, in addition to the reduction of pain and swelling in the joints. Isokinetic dynamometry is considered the gold standard for objectifying forces/moments in the knee [19].

In this paper, it is hypothesized that is possible to find a model that reliably predicts knee resistance for a healthy population; the improvement in strength (increase in knee torque) may also imply the follow-up of the patient's improvement during the rehabilitation treatment of the knee.

The possibility of modeling knee force and moment for healthy people may imply the creation of a force and moment reference for diagnoses in patients in the future using the procedure proposed in this paper.

4. Knee joint force and moment models

4.1. Theoretical mechanical model

The cable-driven robot for lower limb movements, Section 2, will be used to collect cable force data for different knee angles. According to Section 3, the human knee is compared to a pulley segment. For the development of the theoretical model, the knee will be considered only as ideal support (friction-free) with free rotation around the transverse axis XX', in the sagittal plane, Fig. 2(a). Another important assumption is that the test is static; that is, there is no motion involved and the acceleration is zero, Eq. (1). The assumption of static tests is made in function of low speeds and accelerations present in the kinematics of human gait rehabilitation [20].

$$\sum \vec{F} = 0; \sum \vec{M} = 0 \tag{1}$$

From the free body diagram, Fig. 3, and the angles shown in Fig. 4, one can find the values of cable force and knee moments for each knee angle from the forces and moments balance.

where

Rx – Knee support reaction on the x-axis;

Ry – Knee support reaction on the y-axis;

$ß$ – Angle of the leg with the vertical, obtained through A_{knee};

Af – Angle of the cable with the vertical, obtained through Beta;

P – Weight of the leg plus the foot, in Newtons;

T – Cable traction force, in Newtons;

t – Total leg dimension;

d – Distance from the place where the cable is connected to the splint to the sole of the foot;

d_{CG} – Distance from the center of the mass of the leg plus foot;

https://doi.org/10.1017/S0263574723000024 Published online by Cambridge University Press

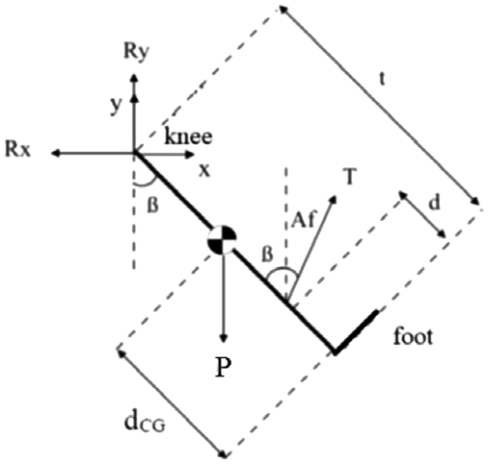

Figure 3. *Free body diagram considering leg + foot.*

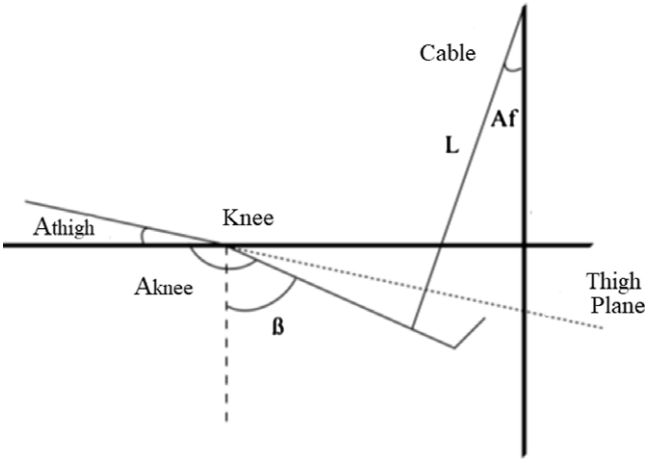

Figure 4. *Detailing of the angles and cable coupling in the leg.*

A_{thigh} – Angle of the thigh;
A_{Knee} – Angle of the leg with the thigh, reproduces the angle of the knee;
L – Initial cable length.

From the initial values – represented by the "$_{\text{ini}}$" – of thigh angle (which remains constant during the test), knee angle, and cable angle, it is possible to calculate the cable angle for any leg position by Eq. (2).

$$Af = tg^{-1}\left[\begin{array}{c}\cos(A\text{thigh} - A\text{Knee}_{\text{ini}} + 180^\circ)\,(t-d) + \\ \dfrac{tg(Af_{\text{ini}})\,L\cos(Af_{\text{ini}}) - \sin(\beta)(t-d)}{L\cos(Af_{\text{ini}}) - \sin(A\text{thigh} - A\text{Knee}_{\text{ini}} + 180^\circ)} \\ (t-d) + \cos(\beta)(t-d)\end{array}\right] \tag{2}$$

where β is given by Eq. (3).

$$\beta = A_{\text{Knee}} - A_{\text{thigh}} - 90^\circ \tag{3}$$

https://doi.org/10.1017/S0263574723000024 Published online by Cambridge University Press

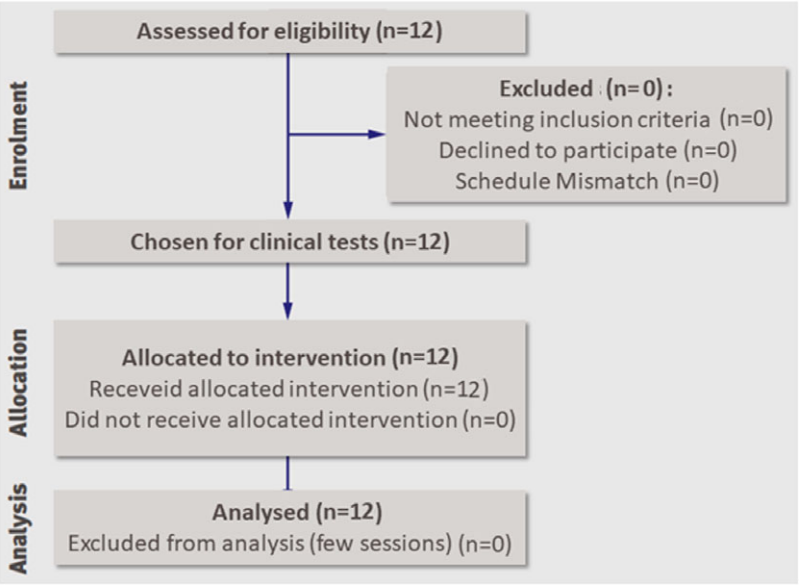

Figure 5. *Flow diagram of the clinical tests with healthy subjects.*

Solving the static equilibrium given in Eq. (1) for the x and y axes is possible to obtain:

$$\sum Fx = 0 \rightarrow Rx - Tx = 0 \rightarrow Rx = Tx = T\sin(Af) \tag{4}$$

$$\sum Fy = 0 \rightarrow Ry + Ty - P = 0 \rightarrow Ry = P - Ty = P - T\cos(Af) \tag{5}$$

The point where the foot meets the leg is used to calculate the equilibrium of moments in the system, as in Eq. (6).

$$Ry\sin(\beta)t - Rx\cos(\beta)t - P\sin(\beta)d_{\mathrm{CG}} + T\sin(\beta + Af)\,d = 0 \tag{6}$$

Isolating T in Eq. (6), one has:

$$T = \frac{P\sin(\beta)(t - d_{\mathrm{CG}})}{\sin(\beta + Af)(t - d)} \tag{7}$$

In this way, it is possible to calculate the theoretical force in the cable at each position of the leg, Eq. (7). The resulting theoretical moment is then the sum of the moments of Rx and Ry, as in Eq. (8), where MjT is the total moment at the theoretical knee.

$$MjT = (P - T\cos(Af))\sin(\beta)t - T\sin(Af)\cos(\beta)t \tag{8}$$

4.2. Biomechanical model

In the real case, it is known that the knee offers resistance to movement due to ligaments, muscles, and friction between bones, among others. This real knee resistance implies an experimental moment that will be called Me. In this way, the total moment in the experimental knee will be the sum of the theoretical moment previously calculated, Eq. (8), with the unknown experimental moment Me, where MjE is the total moment in the experimental knee.

$$MjE = MjT + Me \tag{9}$$

https://doi.org/10.1017/S0263574723000024 Published online by Cambridge University Press

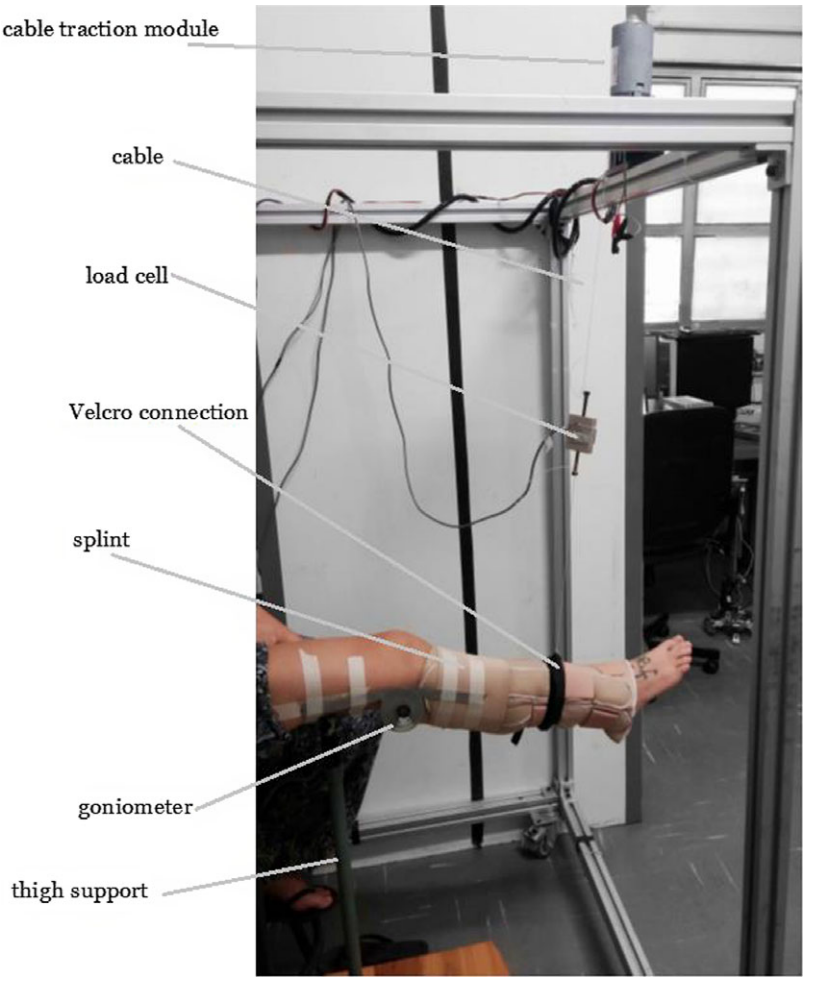

Figure 6. *Experimental setup.*

As *Me* is unknown, to calculate *MjE*, the moment balance around the foot-to-leg point contact is performed again, Eq. (10).

$$\sum \vec{M} = 0 \rightarrow MjE = P\sin(\beta)d_{CG} - T\sin(\beta + Af)d \tag{10}$$

With Eq. (10) and the cable force data for each leg angle, one can then calculate the experimental moment for each angle. The calculation of the experimental moment is done indirectly from the traction force measured by the load cell, Eq. (10).

4.3. Experimental methodology

The Research Ethics Committee of the UFU (Brazil) approved this study (CAAE N° 51133821.4.0000.5152), and written informed consent was obtained before any data collection. To participate in the tests, volunteers had to be between 15 and 30 years old, have a body mass of up to 100 kg, be sedentary (practice physical activity at most once a week), and not have had problems with arthrosis, dislocations, or knee and hip operations. Tests were performed on 6 men and 6 women.

The flow diagram of the clinical test with healthy subjects is shown in Fig. 5.

https://doi.org/10.1017/S0263574723000024 Published online by Cambridge University Press

Table III. *Data statistics of the subjects.*

	Average	**Standard deviation**	**Average**	**Standard deviation**	**Average**	**Standard deviation**
	Female		**Male**		**Total**	
Gender	50%	–	50%	–	–	–
Age (years)	22.500	3.209	21.167	2.317	21.833	2.758
Dominant leg	Right = 100%	Left = 0%	Right = 83.3%	Left = 16.7%	Right = 91.7%	Left = 8.30%
Frequency of physical activity	Never = 75.0%		1 time a month = 16.7%		2 times a month = 8.30%	
Mass (kg)	60.817	13.699	66.533	13.729	63.675	13.412
Leg + foot mass (kg)	4.063	0.915	4.112	0.848	4.087	0.842
Leg size (cm)	44.167	1.204	50.083	2.352	47.125	3.567
CM leg + foot (cm)	24.998	0.682	28.347	1.331	26.673	2.019
Distance from cable to foot (cm)	16.000	0.837	18.133	1.344	17.067	1.543
Thigh						
Circumference (cm)	48.567	5.269	45.850	5.893	47.208	5.515
Qty fat (mm)	36.833	14.289	21.889	8.926	29.361	13.781
Calf						
Circumference (cm)	36.333	2.714	35.750	3.142	36.042	2.816
Qty fat (mm)	24.083	12.147	13.283	6.899	18.683	10.978

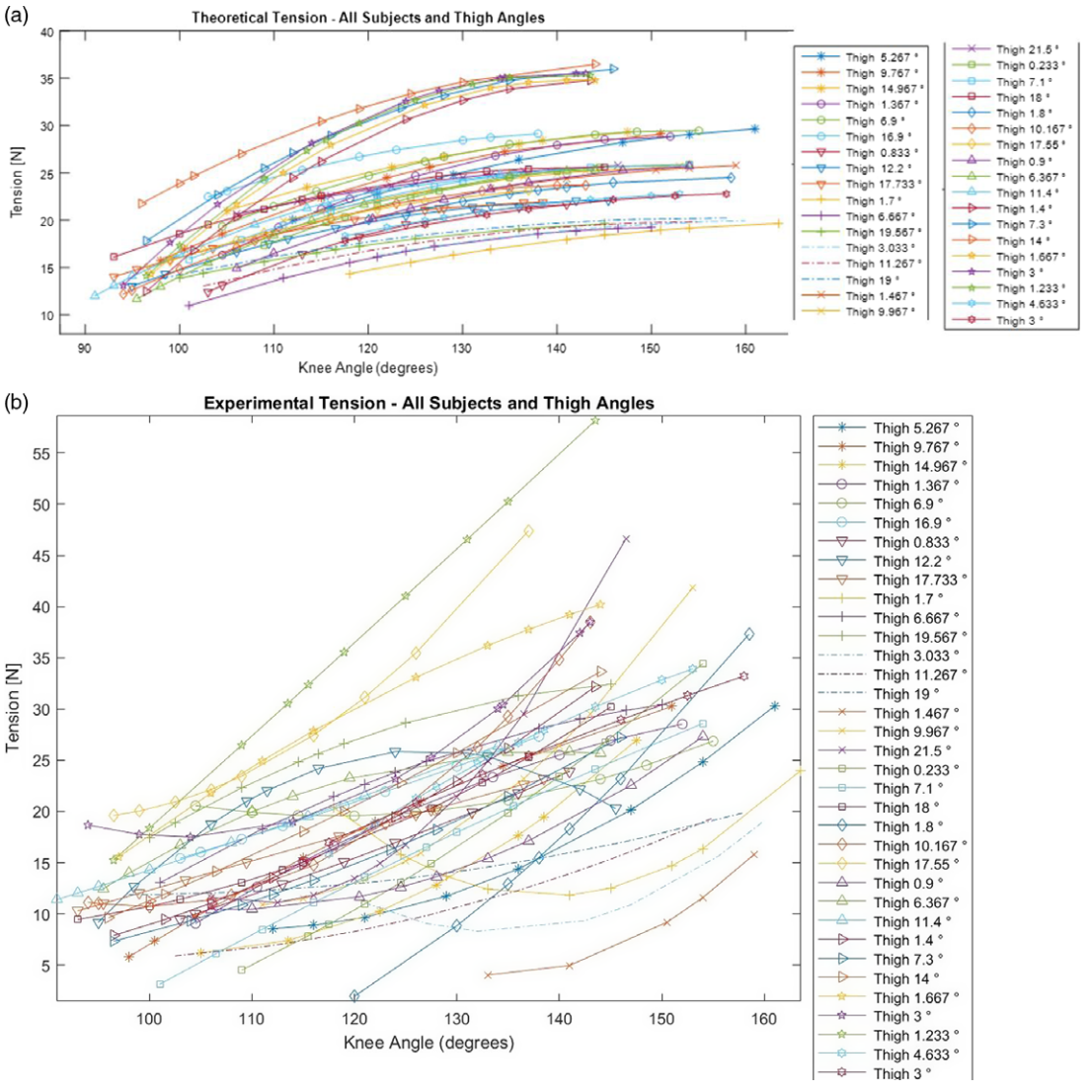

Figure 7. *(a) Theoretical knee cable forces all tests; (b) Experimental knee cable forces all tests.*

Two procedures were created: the first was to test 10 individuals from the population, and the second was to test the two remaining subjects. The first protocol tested three thigh angles, Fig. 6, (the first between 0° and 5°, the second from 5° to 10°, and the last from 10° to 15°) only in the descent movement, that is, flexion of the knee. The second tested the same thigh angle (around 0°) in three phases of descent and ascent, working on knee flexion and extension.

The general testing protocol included the following:

- Completion of a questionnaire with age, gender, race, frequency of physical activity, and body mass (measured with a Plenna Ice scale with a minimum capacity of 10 kg and a maximum of 150 kg and graduation of 100 g);
- Test only on the dominant leg;

https://doi.org/10.1017/S0263574723000024 Published online by Cambridge University Press

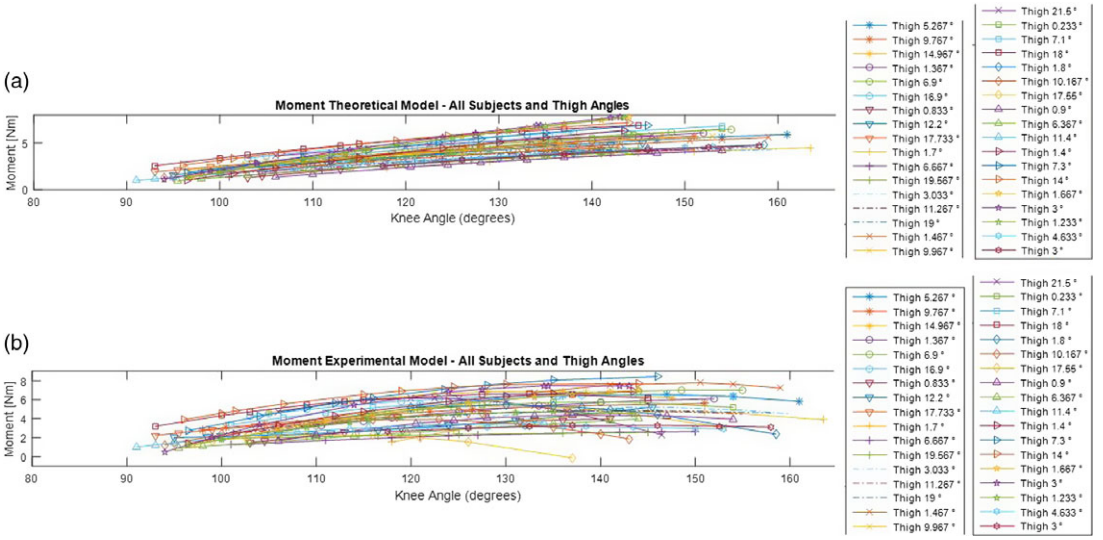

Figure 8. *(a) Theoretical knee moments; (b) Experimental knee moments.*

- Measurement of dominant leg size, the subject should be sitting with feet barefoot on the floor and knee at approximately 90°, the examiner measured the distance from the lateral epicondyle of the femur to the ground with a Cescorf 2 m anthropometric tape measure and 1 mm resolution;
- Measurement of leg circumference and amount of thigh and calf fat dominant using a Mitutoyo plicometer with a sensitivity of 0.1 mm and amplitude of 85 mm reading;
- The test should be performed barefoot, to avoid the extra weight of the shoe;
- Placement of the splint and the velcro connection with the cable approximately 10 cm from the lateral malleolus and measuring the distance from the velcro to the sole with the tape measure anthropometric;
- A position to sit in the chair in which the subject remained upright was standardized over the hip, extra support was used to keep the thigh at the same level during the whole experiment.

For each thigh angle, a test was performed:

- The thigh angle was then measured with an M-D SmartTool digital inclinometer Building Products with 1/10th of a degree resolution, and also the cable start angle;
- The initial length of the cable up to the fastening velcro was measured with the tape measure anthropometric;
- The knee angle was measured with a Mitutoyo goniometer with a range from 0 to 90° and a resolution of 1°, and, after about 1 min in position, the force in the cable was measured by the cable-driven robot, 10 measurements were obtained and an average was used for load calculations;
- The examiner operates the robot, the leg descent, and repeated the previous step until the maximum flexion, so the examiner changed the angle of the thigh and repeated the process.

In the case of the second procedure, after the complete descent, the examiner collected the cable to different angles of extension, also measuring the force in the cable at each of these.

Figure 6 shows in detail the coupling of the goniometer on the leg for reading knee angles and the velcro connection on the splint to attach the cable to the individual's leg, and the subjects were positioned in the same way using the thigh support, Fig. 6.

https://doi.org/10.1017/S0263574723000024 Published online by Cambridge University Press

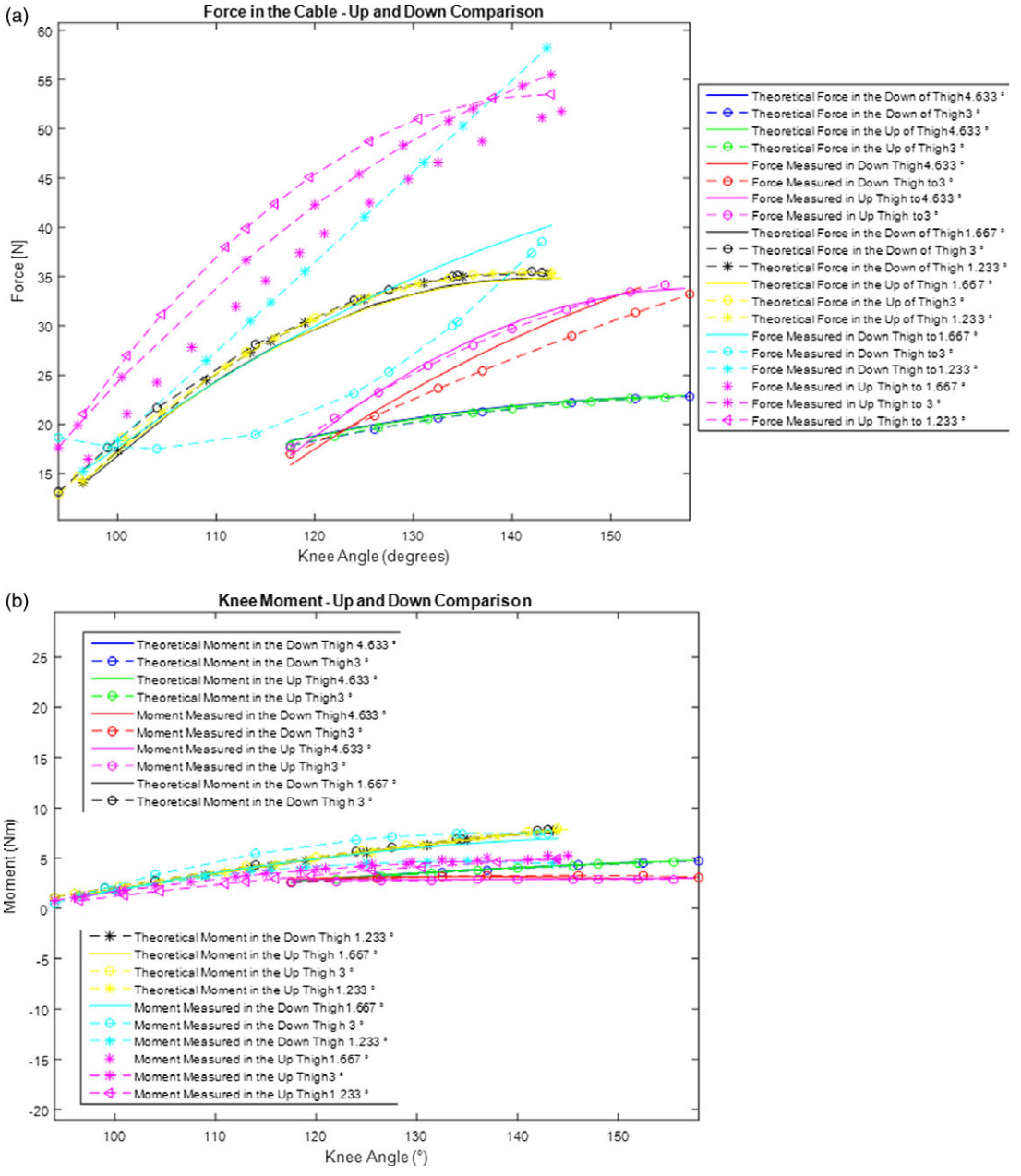

Figure 9. *(a) Cable forces for up and down in two subjects; (b) Knee moments for up and down in two subjects.*

5. Results and discussion

Table III shows the data statistics for the entire population and separation by male and female.

Tests lasted about an hour for each subject, and no repetitions were done, to avoid the physical and psychological fatigue of the subject, which could affect the data collected [18].

https://doi.org/10.1017/S0263574723000024 Published online by Cambridge University Press

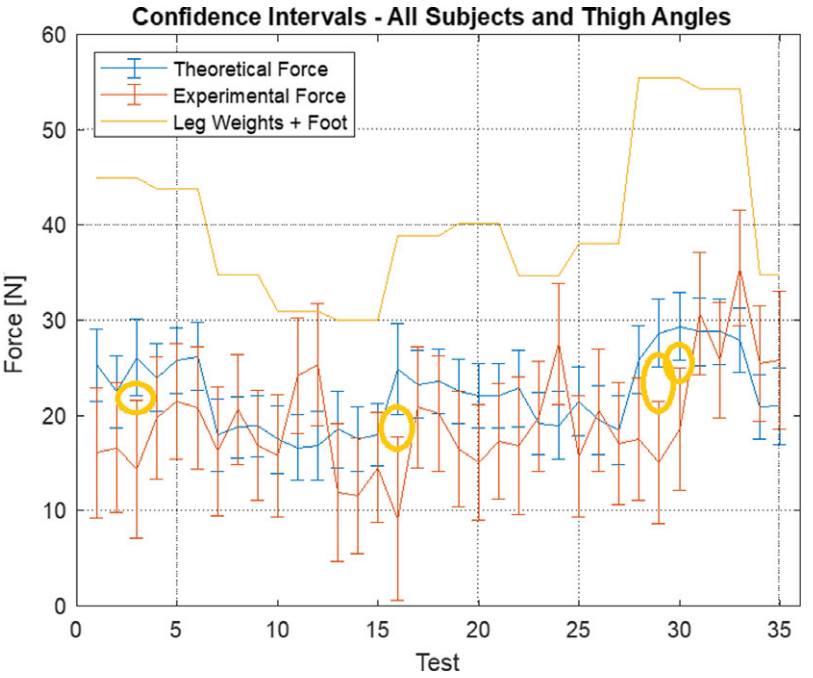

Figure 10. *ANOVA test for all subjects and thigh angles.*

5.1. Theoretical versus experimental force and moment

Theoretical knee versus experimental cable force (tension), Fig 7, and theoretical knee moment data versus experimental, Fig. 8, were plotted for all ascend tests. The data obtained are fitted to a polynomial curve of order 2.

General trends of the theoretical data can be seen in Figs. 7(a) and 8(a). Each symbol refers to an individual, and it is possible to see that the curves of the same individual remain close, indicating a greater influence of the weight of the lower limb on the curve and little influence of the angle of the thigh itself.

For the experimental data, Figs. 7(b) and 8(b), there is still the presence of some tendency in the curve shape, although there are some very different curves from this trend. This could indicate that each subject can have a curve with different trends, which can occur for various reasons such as reading errors, failure to relaxation the individual, or even some greater resistance encountered at an angle specific that does not necessarily imply an error. Statistical treatment is necessary to draw deeper conclusions, which will be presented in item 5.3.

During the performance of the tests on the cable-driven robot, there was a difference between ascent (knee extension) and descent (flexion) movement. In theory, both movements would be equal and therefore would have the same force and moment results at the knee. To experimentally verify the performance of the force in these cases, tests were performed on two volunteers (a man performed three descent and ascent tests, and a woman performed two tests due to the long experimentation time), Fig. 9.

5.2. Flexion and extension movement

The theoretical force data for the descent and ascent were the same obviously, Fig. 9(a). In the experimental force values, it can be seen that the values descents are normally smaller than those on the

https://doi.org/10.1017/S0263574723000024 Published online by Cambridge University Press

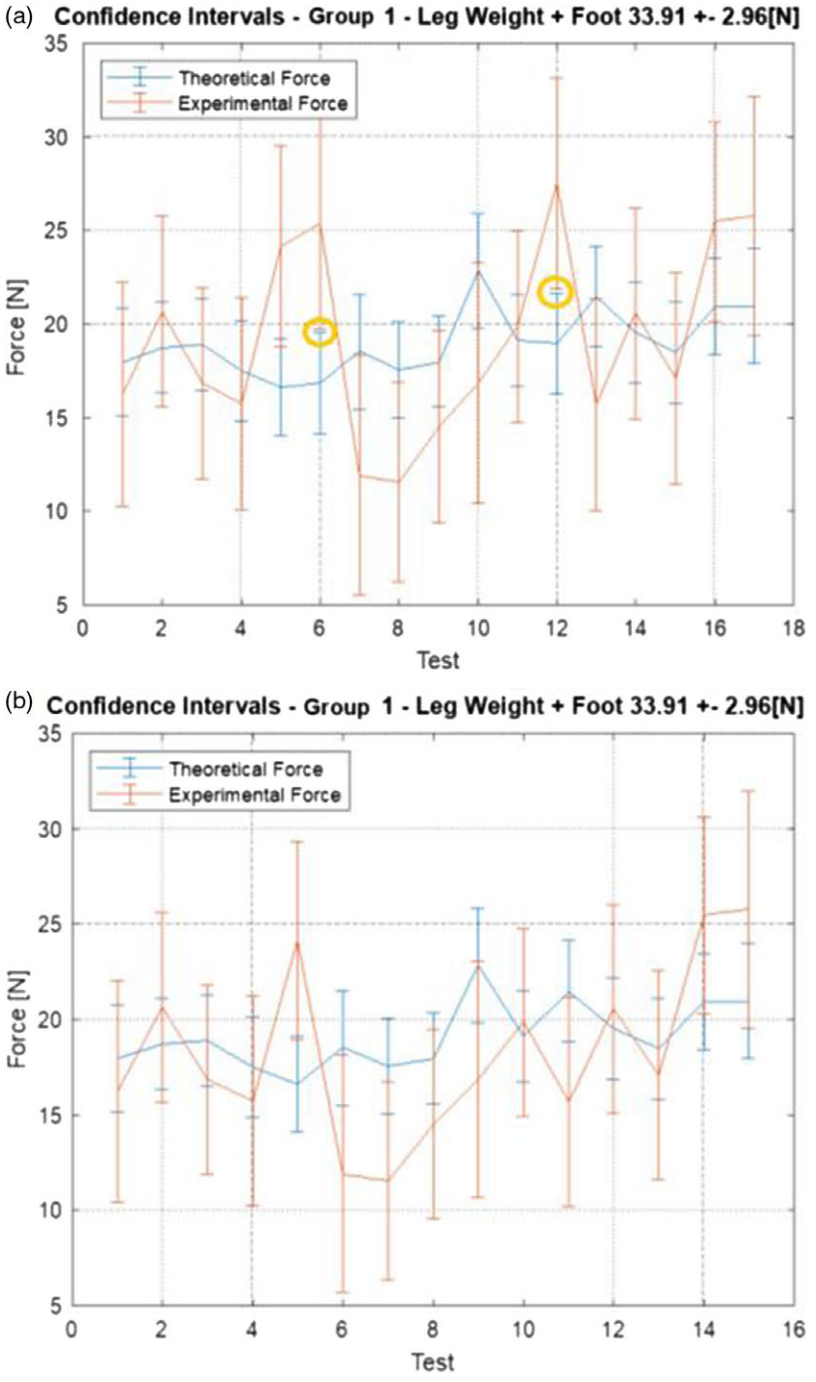

Figure 11. *ANOVA for group* 1*, without test cut (a) and after the cut (b).*

ascent, which means that the moment at the knee varies depending on the extension-flexion movement. The load cell hysteresis could be a reason for such a difference, but the reading of force data was always performed after a certain stop time in a given position, which would eliminate hysteresis. This effect may be intrinsic to the knee itself and may be analyzed further in future works.

https://doi.org/10.1017/S0263574723000024 Published online by Cambridge University Press

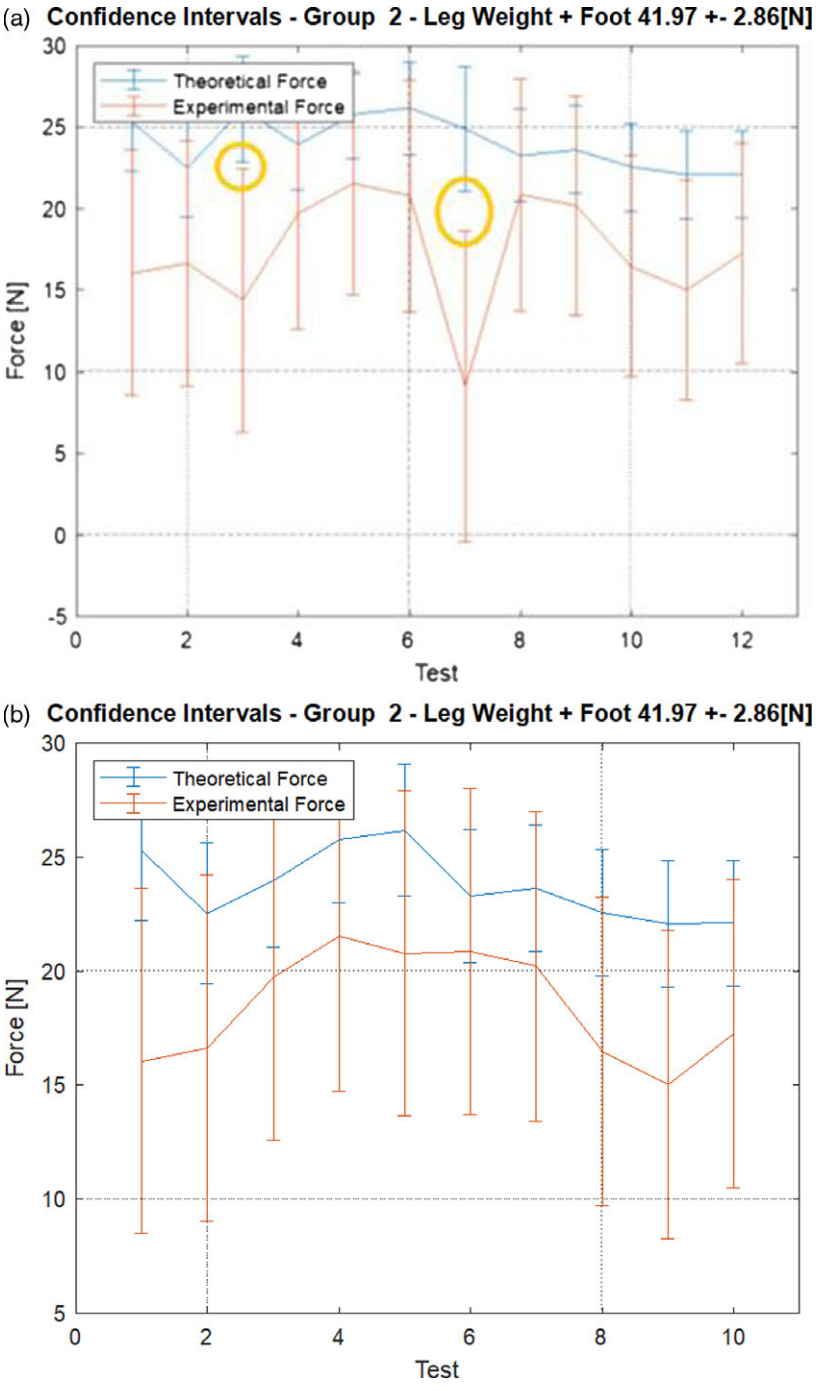

Figure 12. *ANOVA for group* 2*, without test cut (a) and after the cut (b).*

5.3. Statistical analysis: ANOVA test

To more reliably analyze the test data on subjects, an ANOVA test [21] on the entire data group was made. It was considered that the sampling is random and independent, being representative following a normal distribution.

https://doi.org/10.1017/S0263574723000024 Published online by Cambridge University Press

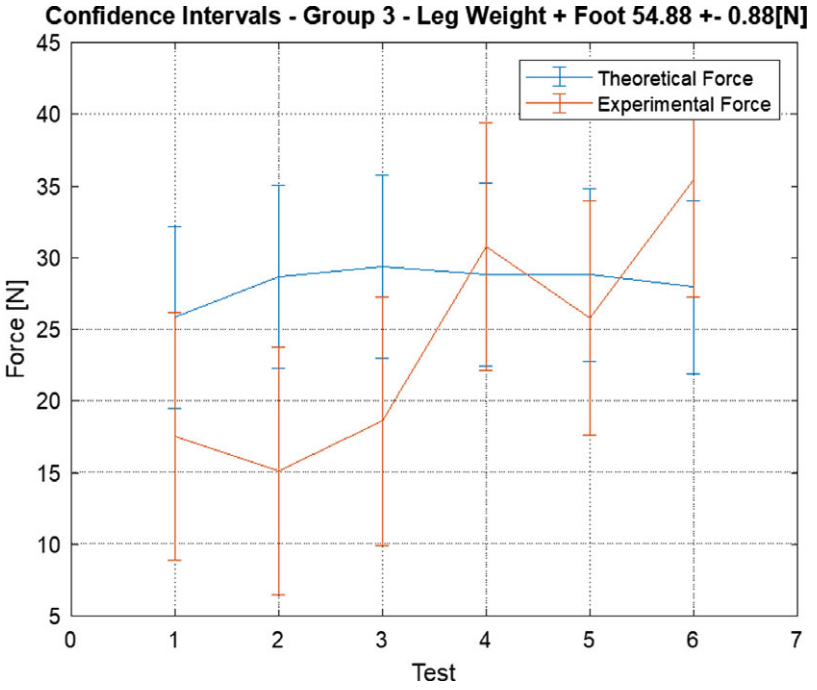

Figure 13. *ANOVA for group 3 without test cut.*

The test was performed on the force data only since the moment depends on the force. A confidence interval of 99% is used, because there are several uncontrollable error sources in the system, such as the possibility of movement of the individual, in addition to the non-relaxation of the muscles by the individual.

Figure 10 shows the graphs for the entire group, where the blue graph refers to theoretical data, the red to experimental data, and the yellow to mass data from the leg + foot in Newtons. The yellow circles show the points where the theoretical average does not find the experimental mean, which occurred in 4 of the 35 tests (11.42% of the tests).

The result obtained, Fig. 10, shows that the theoretical mean follows the mass variation, which indicates that individuals can be separated into groups by mass. Another important factor is that only 11.42% of tests are not represented by the theoretical model which is a value small for an ideal theoretical model (without considerations of friction, viscosity, and others); with some adjustments, these points can be representative, and the model will be more reliable. Among these adjustments, we can mention the addition of the friction effect between the bones in the knee, and the elastic and viscous effects of the knee components, together with the prediction of a theoretical moment that is most significant, among others.

Separating the subjects into three groups concerning the mass of the leg plus the foot, we have Figs. 11 (leg plus foot mass set of 33.91 ± 2.96 [N]), Fig. 12 (leg plus foot mass set of 41.97 ± 2.86 [N]), and Fig. 13 (leg plus foot mass set of 54.88 ± 0.88 [N]).

For group 1, Fig. 11(a) shows the ANOVA for subjects 3, 4, 5, 8, 9, and 12, and the bottom shows the ANOVA with tests 6 and 12 cutoff. The theoretical averages compared to each other are not equal, $(F = 2.5526) > (Fc = 2.1312)$, but they get pretty close when we remove data 6 and 12, resulting in $(F = 2.4928) > (Fc = 2.2289)$, Fig. 11(b). Any adjustment to the theoretical curve or separation of the groups by other factors could cause a decrease in the differences in the means, of passing the test for that set. Even after cutting the experimental data, when compared the experimental average values are not equal, with $(F = 4.4362) > (Fc = 2.2289)$. This may imply that group separation by mass cannot be the best solution; other factors must be studied to improve the distribution of subjects in groups.

https://doi.org/10.1017/S0263574723000024 Published online by Cambridge University Press

In group 2, Fig. 12(a), of subjects 1, 2, 6, and 7, the, theoretical data compared to each other and experimental data related to each other are approved even before cutting with ($F = 2.0817$) < ($Fc = 2.4445$) and ($F = 1.3869$) < ($Fc = 2.4445$), respectively. In this way, this mass separation is validated as representative of the entire population. Even so, contrasting the theoretical data with the experimental results, two non-equal mean points are obtained, which indicates that the model does not fully represent the sample. The cut of tests 3 and 7 are shown in Fig. 12(b), making the group represented by the model developed.

Finally, the third group, Fig. 13, constituted by subjects 10 and 11, has no theoretical average points different from the experimental average and therefore not cut. The results show that the subjects' theoretical averages forces compared were approved with ($F = 0.2812$) < ($Fc = 3.4077$), but the experimental one has large differences from ($F = 6.6373$) > ($Fc = 3.4077$). To improve these results, we can suggest the development of a more complex model or the separation of groups by other factors.

6. Conclusion

Through all the data acquired, it was possible to conclude that the theoretical model developed, however simple it may be due to its hypothesis that the knee has only support components and no friction, is valid for 88.58% of tests performed in ANOVA test analysis with a 99% confidence interval. The high confidence interval can be lowered by developing a more complex theoretical model that may be made up of other variables not controlled as the individual's age, physical activity level, muscle tone, stretching, friction between bones, and elastic and viscous effects on the knee, and other factors that may change the constitution of the knee components.

From the ANOVA test, it was observed that there are no large differences between males and females, and the weight of the lower limb appears to have a greater influence on cable force than other factors such as age, and gender, among others. In mechanical way, this conclusion is function of the mass of the limb is the only force contrary to the force in the cable. This may also indicate that the knee behaves similarly for the entire population, regardless of their individuality. Graphics with similar shapes were also observed in the cable forces and knee moments data, which contribute to the conclusion of similar behavior for the entire population.

Another observed factor of the study was that there are differences between ascent (extension) and descent (flexion) movements that need to be studied further in future works.

This theoretical model implies a theoretical moment of reference that can help the examiner to assess the patient's situation throughout the treatment, in addition to its improvement over time. The use of the cable-driven robot presented in this paper can be a low-cost alternative when compared to isokinetic dynamometry.

The representativeness of the proposed model to a healthy population is verified, enabling the building of a reference for comparison with patients in the future. The next steps of this work are the comparison of the proposed model with others presented in the literature, dynamic measurements with the cable-driven robot, and experimental tests with patients.

Data availability statement. There are no additional files. All necessary data have been included in the body of the text.

Author contributions. The authors contributed equally to the preparation of the paper.

Financial support. This work was supported in part by CNPq under Grant 03511/2021-4, CAPES (Finance code 001) and FAPEMIG under Grant APQ-02829-17.

Conflicts of interest. The authors declare none.

Ethical approval. Experimental trials have been approved by the ethics committee on human research at the Federal University of Uberlândia (CAAE N° 51133821.4.0000.5152).

References

[1] G. Zuccon, B. Lenzo, M. Bottin and G. Rosati, "Rehabilitation robotics after stroke: A bibliometric literature review," *Expert Rev. Med. Devices* **19**(5), 405–421 (2022). doi: 10.1080/17434440.2022.2096438.

[2] C. Duret, A-G. Grosmaire and H. I. Krebs, "Robot-assisted therapy in upper extremity hemiparesis: Overview of an evidence-based approach," *Front. Neurol.* **10**, 412 (2019). doi: 10.3389/fneur.2019.00412.

[3] R. S. Gonçalves, J. C. M. Carvalho, J. F. Ribeiro and V. V. Salim, "Cable-Driven Robot for Upper and Lower Limbs Rehabilitation," **In:** *Handbook of Research on Advancements in Robotics and Mechatronics*, 1st edn. (IGI Global, Cairo, 2015) pp. 284–315.

[4] B. Hobbs and P. Artemiadis, "A review of robot-assisted lower-limb stroke therapy: Unexplored paths and future directions in gait rehabilitation," *Front. Neurorobot.* **14**, 19 (2020). doi: 10.3389/fnbot.2020.00019.

[5] L. Tappeiner, E. Ottaviano and M. L. Husty, "A Cable-Driven Robot for Upper Limb Rehabilitation Inspired by the Mirror Therapy," **In:** *Computational Kinematics, Mechanisms and Machine Science*, vol. 50 (Springer, Cham, 2018) pp. 174–181.

[6] H. Xiong and X. Diao, "A review of cable-driven rehabilitation devices," *Disabil. Rehabil. Assist. Technol.* **15**(8), 885–897 (2020). doi: 10.1080/17483107.2019.1629110.

[7] T. Alves, R. S. Gonçalves and G. Carbone, "Serious games strategies with cable-driven robots for bimanual rehabilitation: A randomized controlled trial with post-stroke patients," *Front. Robot. AI* **9**, 1–22 (2022). doi: 10.3389/frobt.2022.739088.

[8] S. J. Hall, *Basic Biomechanics*, 7th ed. (Mc-Graw-Hill, New York, 2014).

[9] A. M. Barbosa, J. C. M. Carvalho and R. S. Gonçalves, "Cable-driven lower limb rehabilitation robot," *J. Braz. Soc. Mech. Sci. Eng.* **40**(5), 245 (2018).

[10] T. Alves, M. C. Carvalho and R. S. Gonçalves, "Assist-as-needed control in a cable-actuated robot for human joints rehabilitation," *J. Mech. Eng. Biomech.* **5**(3), 57–62 (2019).

[11] I. Kapandji, *Physiology of the Joints: Lower Limb*, 6th ed. (Churchill Livingstone, Edinburgh, 2010).

[12] M. Waldén and M. Hagglund, "Knee injuries – diagnostics, treatment and prevention," *Dansk Sportsmedicin* **4**, 16 (2012).

[13] F. Nardini, C. Belvedere, N. Sancisi, M. Conconi, A. Leardini, S. Durante and V. Parenti-Castelli, "An anatomical-based subject-specific model of in-vivo knee joint 3D kinematics from medical imaging," *Appl. Sci.* **10**(6), 2100 (2020). doi: 10.3390/app10062100.

[14] M. Olinski, A. Gronowicz and M. Ceccarelli, "Development and characterization of a controllable adjustable knee joint mechanism," *Mech. Mach. Theory* **155**, 104101 (2021). doi: 10.1016/j.mechmachtheory.2020.104101.

[15] S. Plagenhoef, F. G. Evans and T. Abdelnour, "Anatomical data for analyzing human motion," *Res. Q. Exerc. Sport* **54**(2), 169–178 (1983); *Proceedings - 9th International Conference on Rehabilitation Robotics*, pp. 430–433.

[16] W. T. Dempster, *Space Requirements of the Seated Operator* (Wright Air Development Center. TIA-55-159, Wright-Patterson Air Force Base, Ohio, 1955) (AD 87 892).

[17] D. Neumann and D. Fapta, *Kinesiology of the Musculoskeletal System: Foundations for Rehabilitation*, 3rd ed. (Mosby, St. Louis, 2016).

[18] H. J. Stam, *Dynamometry of the Knee Extensors; Isometric and Isokinetic Testing in Healthy Subjects and Patients*. Erasmus University Rotterdam (1990, January 3). Retrieved from http://hdl.handle.net/1765/50898

[19] V. Tittelboom, I. Alemdaroglu-Gürbüz, B. Hanssen, L. Heyrman, H. Feys, K. Desloovere, P. Calders and C. Van den Broeck, "Reliability of isokinetic strength assessments of knee and hip using the Biodex System 4 dynamometer and associations with functional strength in healthy children," *Front. Sports Act. Living* **4**, 817216 (2022). doi: 10.3389/fspor.2022.817216.

[20] R. S. Gonçalves and H. I. Krebs, "MIT-Skywalker: Considerations on the design of a body weight support system," *J. Neuroeng. Rehabil.* **14**(1), 1–11 (2017). doi: 10.1186/s12984-017-0302-6.

[21] D. Iacobucci, *Analysis of Variance (ANOVA)* (Independently published, 2020).

Cite this article: R. S. Gonçalves and Y. V. Kaufmann (2023). "Comparison of theoretical and experimental models for knee flexion/extension using a cable-driven robot", Robotica **41**, 1617–1633. https://doi.org/10.1017/S0263574723000024